Broadband RF Phased Array Design with MEEP

Jordan Hanson
Assistant Professor of Physics and Computer Science
July 27, 2022

Department of Physics and Astronomy, Whittier College
Member, IceCube Gen2 Collaboration
Summer Research Fellow with the Office of Naval Research
jhanson2@whittier.edu

Outline

Outline

1. **Background** … *From microns to centimeters: applications of CEM in research with IceCube Gen2 and the Office of Naval Research (ONR)*
2. **Broadband RF Phased Arrays** … *Computations of phased array designs, matching results to theoretical expectations*
3. **Variation of the Index of Refraction** … *Ray-tracing and 3D mapping of RF phased array radiation in non-trivial media*
4. **Progress in RF Antenna Design** … *RF antenna CAD and GDSII import, predicting antenna efficiency and radiation pattern, 3D printing of final products*

Background

Background: Whittier College

- Founded in 1887 in Whittier, California, halfway between DTLA and Anaheim, CA, near East Los Angeles.
- We are a 4-year liberal arts college, and a Title V Hispanic Serving Institution (HSI)
- Departments of Physics and Astronomy, Computer Science, and Mathematics all in Science and Learning Center
- My five research areas: *CEM*, the Askaryan effect (UHE neutrinos), *RF Antenna design and fabrication*, Antarctic ice properties, drones

(Top right): North Quad of Whittier College
(Bottom right): Science and Learning Center

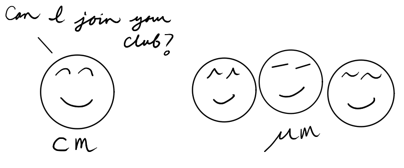

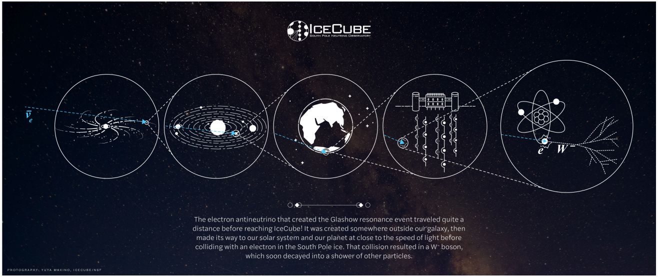

- Largest ultra high-energy neutrino (UHE-ν) detector in the world, via Cherenkov and Askaryan effects. These occur when sub-atomic particles move faster than light in dielectric media.
- Located in glacial ice at the South Pole, properties and volume of ice

---

(Top): High-energy neutrino pathway from (unknown) source to IceCube. (Bottom right): IceCube schematic

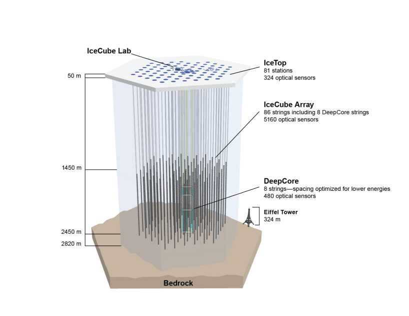

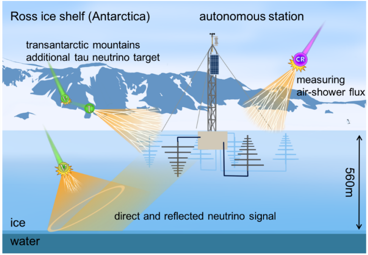

- The Askaryan effect: UHE-ν events generate cascade of charged particles that radiate collectively in the RF bandwidth.
- RF radiation travels for kilometers in Antarctic and Greenlandic ice.
- **RF phased arrays** are used for primary trigger.

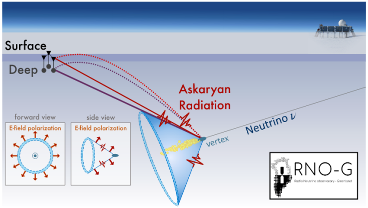

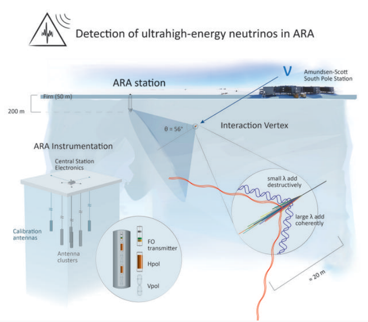

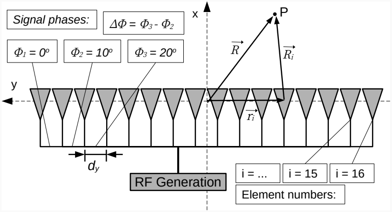

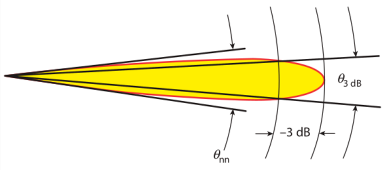

Figure 8-1. This three-dimensional plot shows the strength of the radiation from a pencil beam antenna.

- Office of Naval Research (ONR) is also interested in phased array research: telemetry, targeting, tracking, GPS modernization
- Anechoic chambers used for equipment testing and verification
- Phased arrays (AESAs) can steer radar beams with no moving parts
- We discovered MEEP as an alternative to expensive proprietary RF antenna simulation software

Background: Relevant Links

- *Whittier College* … www.whittier.edu
- *The IceCube Observatory* … https://icecube.wisc.edu
- *The IceCube Collaboration* … https://wipac.wisc.edu
- *Askaryan Radio Array* … https://ara.wipac.wisc.edu/home
- *ARIANNA* … https://ccapp.osu.edu/research/experiments-and-surveys/arianna
- *Radio Neutrino Observatory Greenland* … https://radio.uchicago.edu
- *Office of Naval Research* … https://www.nre.navy.mil
- *Naval Surface Warfare Center (Corona Division)* … https://www.navsea.navy.mil/Home/Warfare-Centers/NSWC-Corona

Broadband RF Phased Arrays

Starting with the literature search:

A. Fedeli, C. Montecucco, and G.L. Gragnani. “Open-Source Software for Electromagnetic Scattering Simulation: The Case of Antenna Design.” Electronics Journal, **8** (12) (2019) (doi:10.3390/electronics8121506).

- NEC family of codes
- gprMax
- OpenEMS
- Meep mentioned, not involved in analysis comparisons, but Python implementation available

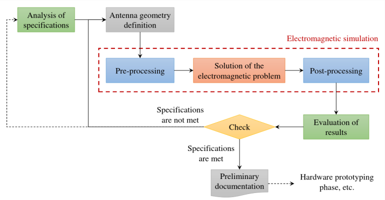

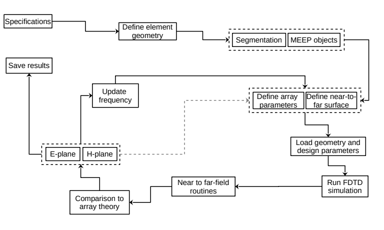

Figure 1: (Left) A. Fedeli *et al* design flow. (Right) From our 2021 work including MEEP.

Inspiration for 2021 paper in the same journal:

Jordan C. Hanson. "Broadband RF Phased Array Design with MEEP: Comparisons to Array Theory in Two and Three Dimensions." Electronics Journal, **10** (415) (2021) (doi:10.3390/electronics10040415).

- Phased array theory
- 1D phased array designs: 2D fields (plus time)
  1. Single-frequency
  2. Broad-band
- 2D phased array designs: 3D fields (plus time)
  1. Single-frequency
  2. Broad-band
- Variation of the index of refraction (Antarctic ice)
- **Won Top 10 Most Notable Articles for the period December 2020 - May 2021.**

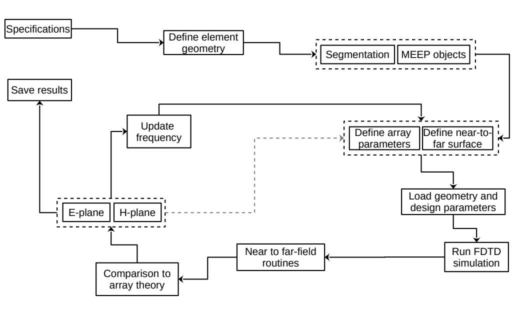

Figure 2: From our 2021 work including MEEP.

MEEP documentation was highly useful:
`https://meep.readthedocs.io/en/latest/`

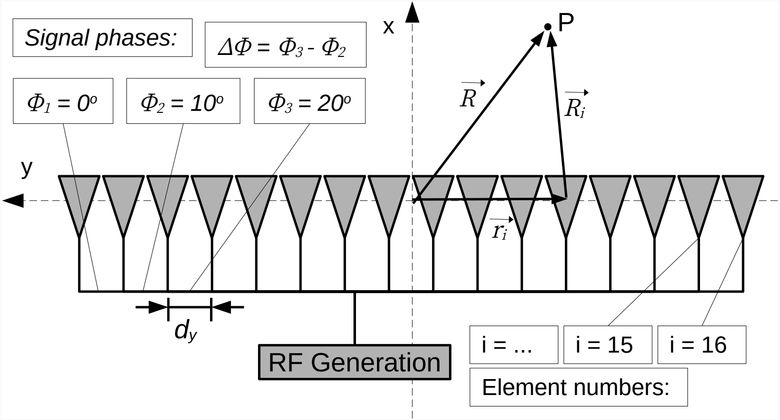

Figure 3: Schematic of *linear* phased array. Let $\Delta\phi$ be the *beam angle*, $\Delta\Phi$ be the phase shift per element, λ be the wavelength, and d_y be the inter-element spacing.

Beam angle and Radiation Pattern

Let λ and d_y be the radiated wavelength and inter-element spacing of a linear phased array. The *beam angle* $\Delta\phi$ of a linear phased array is linearly proportional to the *phase shift per element* $\Delta\Phi$:

$$\Delta\phi = \left(\frac{\lambda}{d_y}\right)\left(\frac{\Delta\Phi}{2\pi}\right) \tag{1}$$

Let $P(\phi)$ be the normalized radiation pattern, or normalized power vs. azimuthal angle, of a linear phased array oriented to radiate in the x-direction. Let ϕ_0 be the beam angle corresponding to $\Delta\Phi = 0$, and let N be the number of elements. The radiation pattern is

$$P(\phi) = \left(\frac{\sin\left(\pi N (d_y/\lambda)(\sin\phi - \sin\phi_0)\right)}{N\sin\left(\pi (d_y/\lambda)(\sin\phi - \sin\phi_0)\right)}\right)^2 \tag{2}$$

The *beam width* (-3 dB points) is $0.886\lambda/L$, where L is the length of the array.

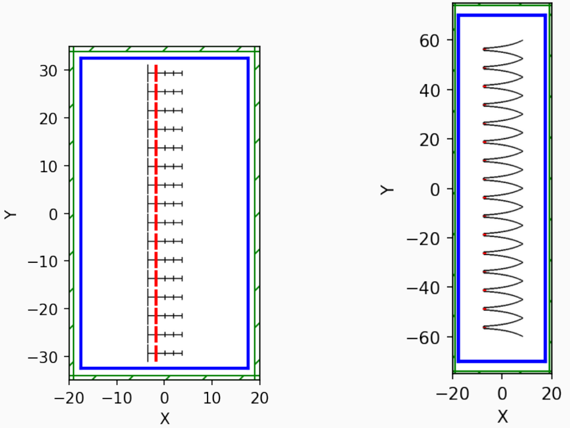

Figure 4: (Left) Yagi-Uda style elements, $N = 16$. (Right) Exponential horn-style elements, $N = 16$. Red elements are Meep **Source** objects, black elements are Meep **GeometricObject** objects. Blue surfaces are Meep **Near2FarRegion** objects. Green surfaces are PML. E-plane radiation pattern in x-y plane, H-plane radiation pattern in x-z plane (3D only).

Broadband RF Phased Arrays: Array and Element Parameters

Yagi-Uda		Horn		SL (dB)			
Parameter	Value	Parameter	Value	f (GHz)	$\Delta\Phi$ (deg)	d_y/λ	SL_{dB}
N	8,16	N	8,16	0.5	80	0.125	-11.6
L	7.2	a	0.95	1.0	80	0.25	-1.2
d_1	1.8	c	15.0	2.0	80	0.5	-1.0
r	3.75	d	3.8	4.0	80	1.0	-0.9
y	2.81	dx	0.1				
z	1.24	$n = c/dx$	150				
d_y	3.92	d_y	$2d$				

Table 1: Yagi-Uda: The first and second columns contain the geometric parameters describing the antenna elements for the Yagi-Uda array. Horn: The third and fourth columns contain those for the horn array. Scan-loss: The fifth through eighth columns contain scan loss data, reported for different frequencies and different d_y/λ values for the $N = 16$ horn array.

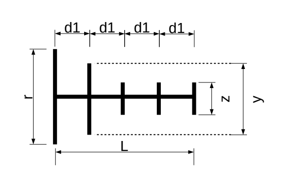

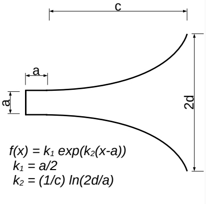

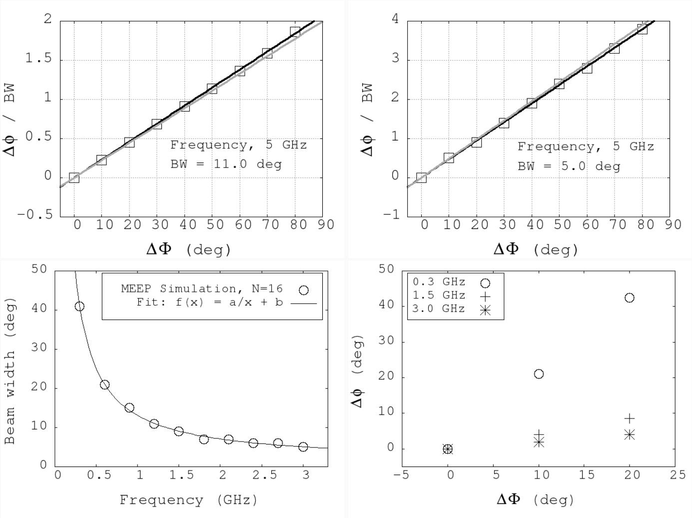

Figure 5: **(Top left)** $\Delta\phi$ divided beamwidth ($N = 8$) 1D Yagi array versus $\Delta\Phi$. **(Top right)** Same, for $N = 16$. **(Bottom left)** Beamwidth vs. frequency for $N = 16$ horn array. **(Bottom right)** $\Delta\phi$ divided beamwidth ($N = 8$) 1D horn array versus $\Delta\Phi$.

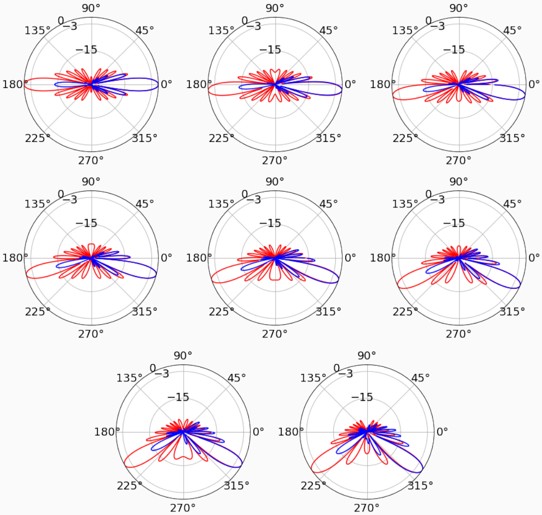

Figure 6: Yagi-Uda 1D $N = 16$ array pattern, for $\Delta\Phi = 0, 10, 20, ..., 70$ degrees (top left to bottom right). Red curves represent Eq. 2, equivalent to row of point sources.

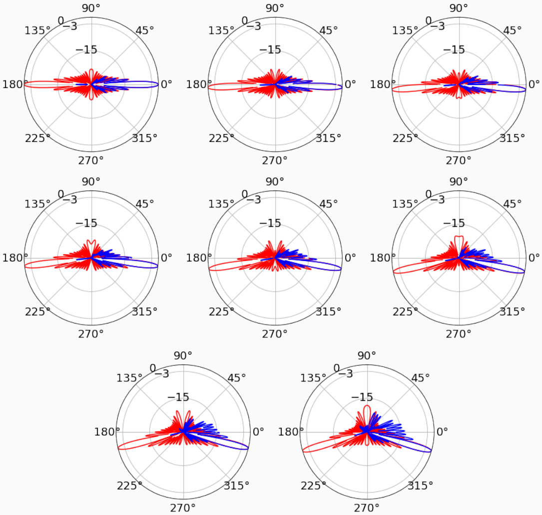

Figure 7: Yagi-Uda 1D $N = 16$ array pattern, for $\Delta\Phi = 0, 10, 20, \ldots, 70$ degrees (top left to bottom right). Red curves represent Eq. 2, equivalent to row of point sources.

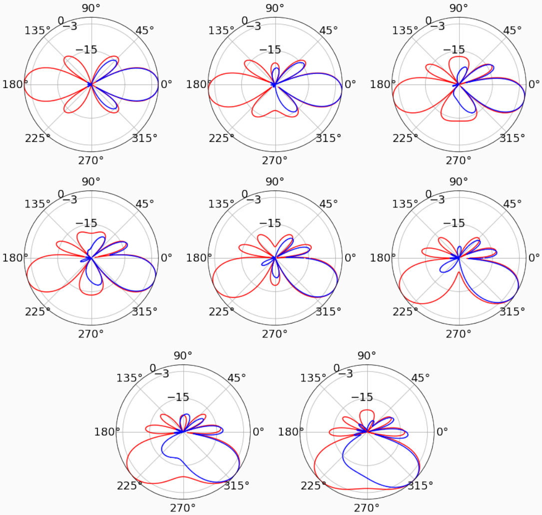

Figure 8: Horn 1D $N = 16$ array pattern, for $\Delta\Phi = 0, 5, ..., 35$ degrees (top left to bottom right). Red curves represent Eq. 2, equivalent to row of point sources.

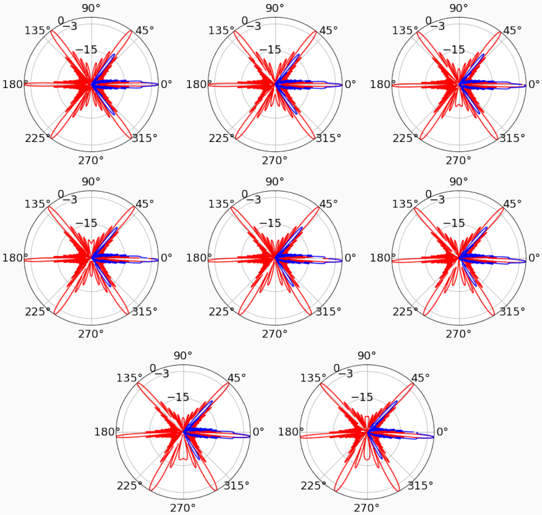

Figure 9: Horn 1D $N = 16$ array pattern, for $\Delta\Phi = 0, 5, ..., 35$ degrees (top left to bottom right). Red curves represent Eq. 2, equivalent to row of point sources.

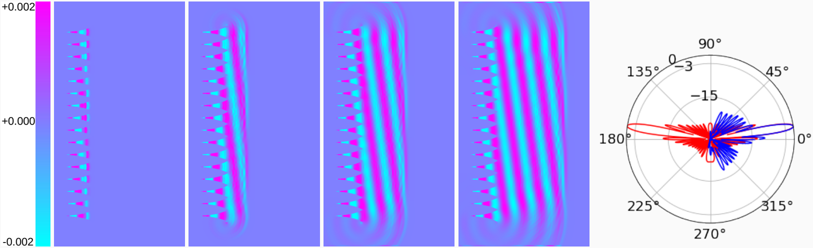

Figure 10: **(From left to right)** The $N = 16$ 1D horn array emitting a linearly polarized electric field at $t = 0.5$ ns, $t = 1.0$ ns, $t = 1.5$ ns, and $t = 2.0$ ns. The area is 80×150 cm^2 (resolution 6), $f = 2.5$ GHz, $\Delta\phi = 9$ degrees from broadside. **(Far right)** The corresponding radiation pattern.

Notes:

- 72 pixels per wavelength, with $\lambda = 12$ cm
- Source is linearly polarized in the y-direction
- Colorscale is $|\vec{E}|$ in the y-direction
- Radiation patterns are obtained from `get_farfield` routine via `Near2FarRegion`

Beam angle and Radiation Pattern

Corollaries to Eq. 1 and Eq. 2 for 2D arrays:

1. The E and H-plane *beam angles* $\Delta\phi_E$ and $\Delta\phi_H$ are linearly proportional to the *phase shifts per element* $\Delta\Phi_E$ and $\Delta\Phi_H$. If the 2D array is a grid that radiates in the x-direction with no phase shifts, then $\Delta\Phi_E$ and $\Delta\Phi_H$ map to the phase shift per column and phase shift per row.
2. Let θ be the zenith angle and ϕ be the azimuthal angle, in a spherical coordinate system. The overall 3D radiation pattern factors into the E and H-plane radiation patterns:

$$P(\theta, \phi) = P(\theta)P(\phi) \tag{3}$$

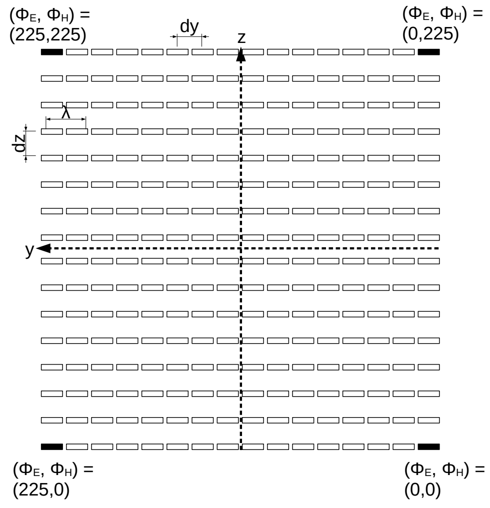

Figure 11: The 2D $N \times N = 16 \times 16$ Yagi-Uda/horn y-polarized array layout. The phase shifts for each row and column are $\Delta\Phi_E = \Delta\Phi_H = 15$ degrees.

Broadband RF Phased Arrays: 2D Array (3D field), array parameters

Yagi-Uda elements needed no modifications for $N \times N = 16 \times 16$.

Horn Array Modifications		
Parameter	Value	System Information
$N \times N$	8×8	Memory consumption
a	2.0	11.7 GB out of 15.5 GB
c	15.0	
d	8.0	CPU cores
dx	0.5	Intel i7 1.80 GHz (8)
$n = c/dx$	30	
d_y	16	MEEP installation
resolution	4	Python3 interface via Conda
backplane location	$-2a$	
backplane thickness	0.5	
backplane dimension	142×142	

Table 2: Parameters for the $N \times N = 8 \times 8$ horn array. The number of CPU cores was 4 in laptop hardware, 8 with hyperthreading. The 8×8 array required 11.7 GB of memory out of 15.5 GB free. The code was written with the Python3 interface to MEEP, installed with the conda package manager, and run in Jupyter notebooks.

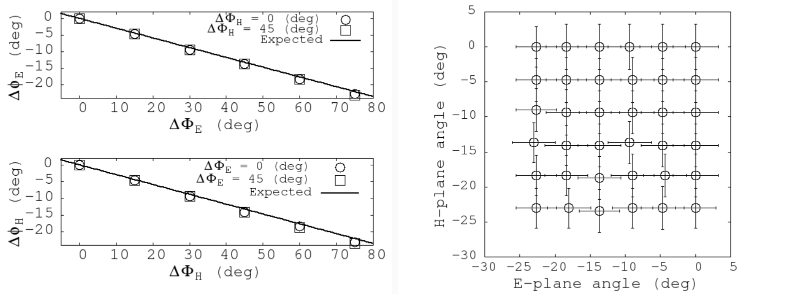

Figure 12: (Left) The beam angles $\Delta\phi_E$ and $\Delta\phi_H$ versus the phase shifts for the $N \times N = 16 \times 16$ Yagi-Uda array at 5 GHz. The black lines represent the theoretical prediction from Eq. 1 ($d_y = d_z$). The circles and squares correspond to two different $\Delta\phi$ constant values for the other array plane. The location of zero phase on the array is chosen to cause a negative beam angle. (Right) The data points correspond to beam angles in the E and H-planes, with the associated beamwidths as errorbars. These data represent one-quarter of the possible scan positions with $\Delta\Phi_{E/H} = 15$ degrees.

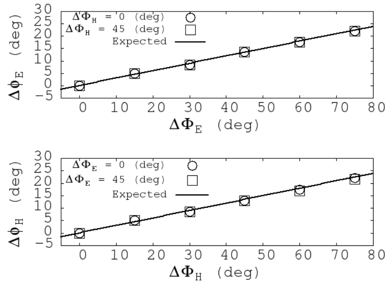

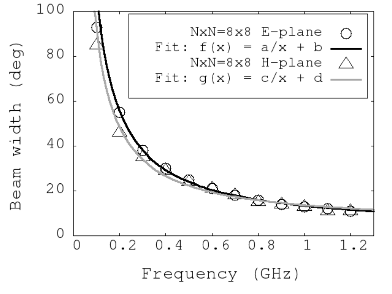

Figure 13: (Left) The beam angles $\Delta\phi_E$ and $\Delta\phi_H$ versus the phase shifts for the $N \times N = 8 \times 8$ horn array at 1 GHz. The black lines represent the theoretical prediction from Eq. 1 ($d_y = d_z$). The circles and squares correspond to two different $\Delta\phi$ constant values for the other array plane. The location of zero phase on the array is chosen to cause a positive beam angle. (Right) The beamwidth in the E and H-planes versus frequency.

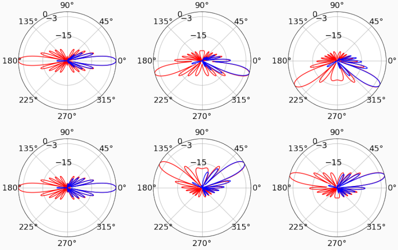

Figure 14: Yagi-Uda 2D array, $f = 3$ GHz. (First row) E-plane ($\Delta\Phi_E$, $\Delta\Phi_H$) = (0, 0) degrees, E-plane ($\Delta\Phi_E$, $\Delta\Phi_H$) = (60, 30) degrees, E-plane ($\Delta\Phi_E$, $\Delta\Phi_H$) = (30, 60) degrees. (Second row) H-plane ($\Delta\Phi_E$, $\Delta\Phi_H$) = (0, 0) degrees, H-plane ($\Delta\Phi_E$, $\Delta\Phi_H$) = (60, 30) degrees, H-plane ($\Delta\Phi_E$, $\Delta\Phi_H$) = (30, 60) degrees.

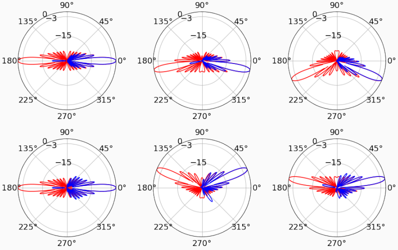

Figure 15: Yagi-Uda 2D array, $f = 4$ GHz. (First row) E-plane ($\Delta\Phi_E$, $\Delta\Phi_H$) = (0, 0) degrees, E-plane ($\Delta\Phi_E$, $\Delta\Phi_H$) = (60, 30) degrees, E-plane ($\Delta\Phi_E$, $\Delta\Phi_H$) = (30, 60) degrees. (Second row) H-plane ($\Delta\Phi_E$, $\Delta\Phi_H$) = (0, 0) degrees, H-plane ($\Delta\Phi_E$, $\Delta\Phi_H$) = (60, 30) degrees, H-plane ($\Delta\Phi_E$, $\Delta\Phi_H$) = (30, 60) degrees.

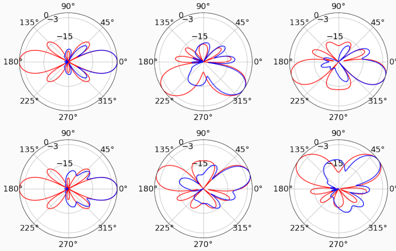

Figure 16: Horn 2D array, $f = 0.5$ GHz. (First row) E-plane ($\Delta\Phi_E$, $\Delta\Phi_H$) = (0, 0) degrees, E-plane ($\Delta\Phi_E$, $\Delta\Phi_H$) = (60, 30) degrees, E-plane ($\Delta\Phi_E$, $\Delta\Phi_H$) = (30, 60) degrees. (Second row) H-plane ($\Delta\Phi_E$, $\Delta\Phi_H$) = (0, 0) degrees, H-plane ($\Delta\Phi_E$, $\Delta\Phi_H$) = (60, 30) degrees, H-plane ($\Delta\Phi_E$, $\Delta\Phi_H$) = (30, 60) degrees.

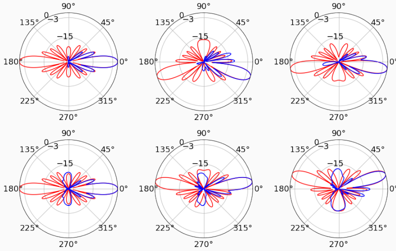

Figure 17: Horn 2D array, $f = 1.0$ GHz. (First row) E-plane ($\Delta\Phi_E$, $\Delta\Phi_H$) = (0, 0) degrees, E-plane ($\Delta\Phi_E$, $\Delta\Phi_H$) = (60, 30) degrees, E-plane ($\Delta\Phi_E$, $\Delta\Phi_H$) = (30, 60) degrees. (Second row) H-plane ($\Delta\Phi_E$, $\Delta\Phi_H$) = (0, 0) degrees, H-plane ($\Delta\Phi_E$, $\Delta\Phi_H$) = (60, 30) degrees, H-plane ($\Delta\Phi_E$, $\Delta\Phi_H$) = (30, 60) degrees.

Variation of the Index of Refraction

Good references for Antarctic index of refraction:

- S.W. Barwick *et al* "Observation of classically 'forbidden' electromagnetic wave propagation and implications for neutrino detection." Journal of Cosmology and Astroparticle Physics **7** (2018) 055. doi:10.1088/1475-7516/2018/07/055.
- J.C. Hanson *et al* "Radar absorption, basal reflection, thickness and polarization measurements from the Ross Ice Shelf, Antarctica." Journal of Glaciology **61** 227 (2015) doi:10.3189/2015JoG14J214.

Simple model derived from snow compaction into solid ice:

$$n(z) = \begin{cases} 1 & z > 0 \\ n_{\mathrm{ice}} - \Delta n \exp(z/z_0) & z \leq 0 \end{cases} \tag{4}$$

Simple model derived from snow compaction into solid ice:

$$n(z) = \begin{cases} 1 & z > 0 \\ n_{\text{ice}} - \Delta n \exp(z/z_0) & z \leq 0 \end{cases} \quad (5)$$

Take-aways:

1. Some component of radiation transmitted horizontally from phased arrays through the “firn” is *shadowed*.
2. There are forbidden incoming trajectories for radiation incident on phased arrays: *shadowing*.
3. We have derived a formula for the expected RF ray trajectory given initial conditions.

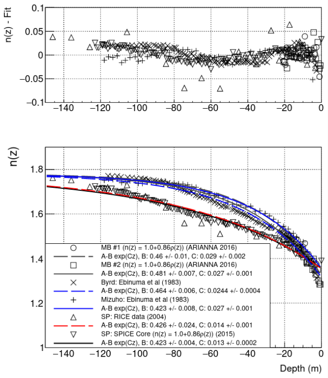

Figure 18: The index of refraction vs. depth for various Antarctic locations.

Simple model derived from snow compaction into solid ice:

$$n(z) = \begin{cases} 1 & z > 0 \\ n_{\text{ice}} - \Delta n \exp(z/z_0) & z \leq 0 \end{cases} \quad (6)$$

Take-aways:

1. Some component of radiation transmitted horizontally from phased arrays through the "firn" is *shadowed*.
2. There are forbidden incoming trajectories for radiation incident on phased arrays: *shadowing*.
3. We have derived a formula for the expected RF ray trajectory given initial conditions.

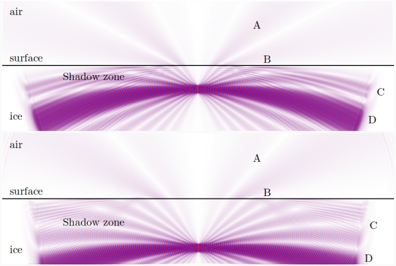

Figure 19: $N = 8$ 1D dipole array, arranged vertically, at $f = 200$ MHz, with dipole length 0.375 m and 0.75 m dipole spacing. Dipoles radiate with z-direction polarization, and the z-component is represented by the color scale. Equation 6 was sampled 100 times vertically ($\Delta z = 0.1$), resolution is 10, and array depths are 15 m (top) and 30 m (bottom), as measured from the top of the array.

Progress in RF Antenna Design

Progress in RF Antenna Design

Open-source design cycle for RF phased arrays:

1. RF antenna CAD and GDSII import with kLayout
    - Begin with functional description of horn structure
    - Generate GDSII file in kLayout
    - Import to Meep for CEM calculations
2. Predicting antenna efficiency and radiation pattern
    - Define voltage standing wave ratio (VSWR) in terms of reflection coefficients (coaxial cable to horn)
    - Use `FluxRegion` objects and coaxial cable model to quantify reflection coefficients
    - Radiation patterns with `Near2FarRegion` objects
3. 3D printing of final products: Multi3D LLC product for 3D printers

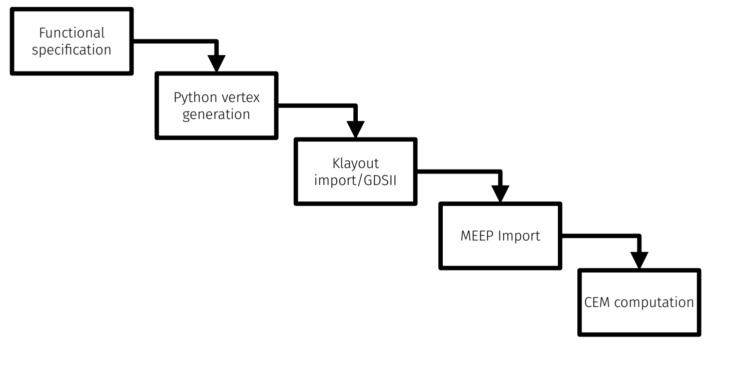

Figure 20: The path to CAD import and CEM with MEEP. (a) Example: functional design of the exponential curve describing the horn. (b) Simple python code to evaluate (x, y) pairs from functional description. (c) Import (x, y) pairs as polygon vertices into kLayout, and save in GDSII format. (d) Import GDSII format as MEEP prisms or volumes (materials or regions). (e) Run computations / visualize with Mayavi.

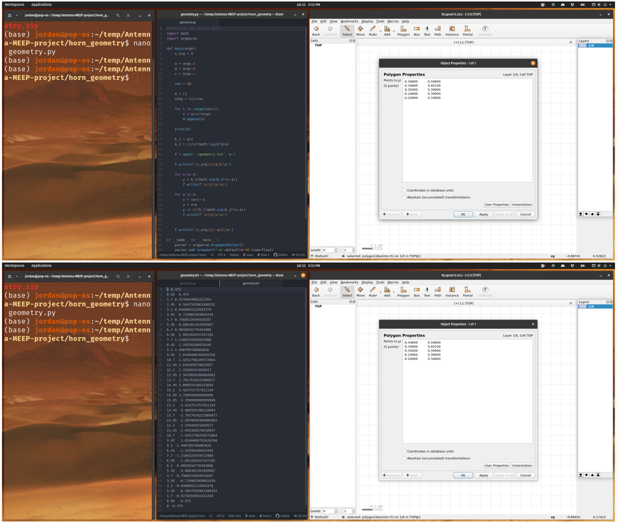

Figure 21: (Top) Run python code (A. Householder, D. Goodman) to generate vertices from functional design. (Bottom) Opening vertex file to copy to klayout polygon.

Progress in RF Antenna Design

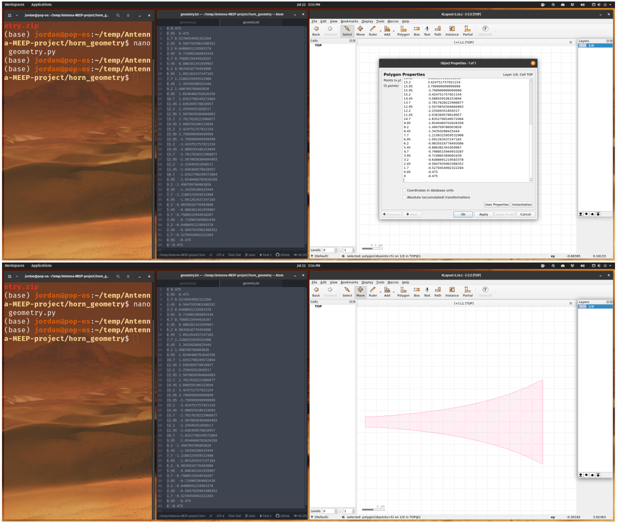

Figure 22: (Top) Vertices imported to klayout. (Bottom) Horn top layer is formed as klayout polygon.

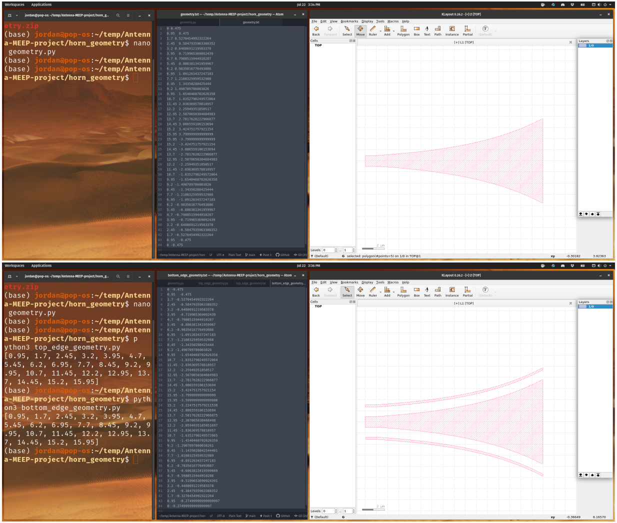

Figure 23: (Top) Horn top layer is formed as klayout polygon. (Bottom) Additional side pieces.

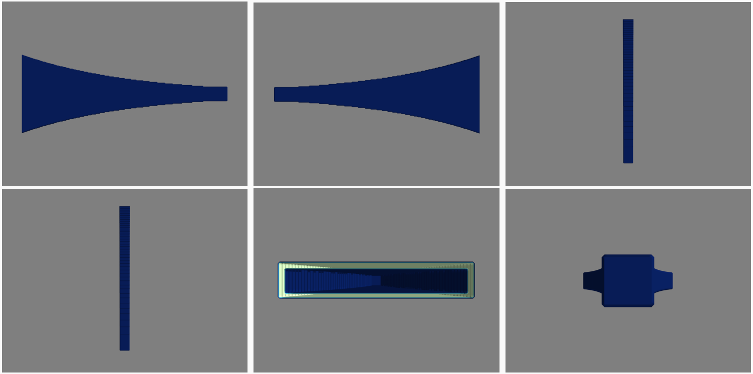

Figure 24: Various views of the horn visualized with Mayavi.

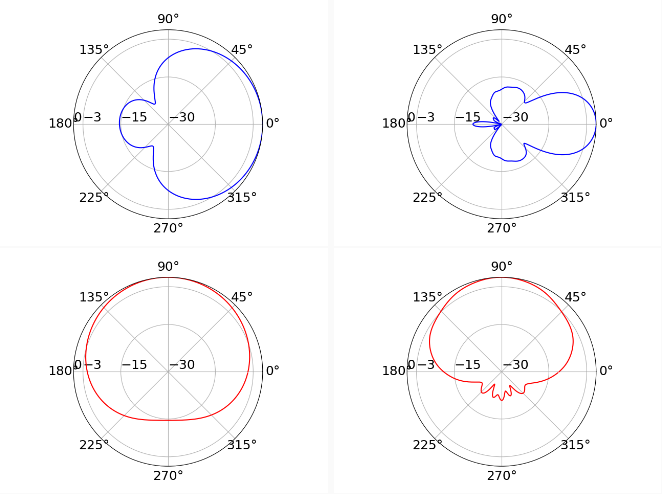

Figure 25: MEEP results for (Top left) E-plane at 0.5 GHz from CAD. (Top right) E-plane at 5.0 GHz from CAD. MEEP results for (Bottom left) H-plane at 0.5 GHz from CAD. (Bottom right) H-plane at 5.0 GHz from CAD.

RF antennas have reflection coefficients. One example from MEEP ReadTheDocs:

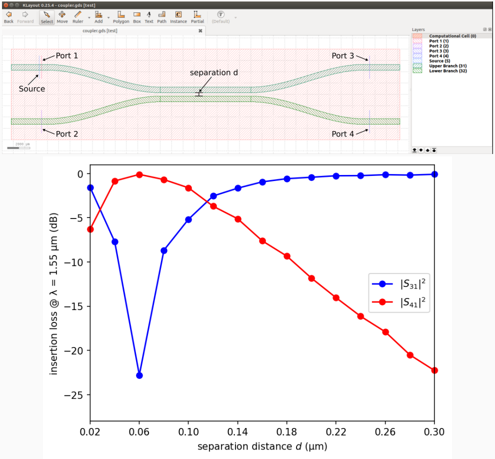

Figure 26: (Top) Directional coupler from kLayout. (Bottom) Reflection/transmission coefficients $|S_{31}|^2$ and $|S_{41}|^2$ (referred to power) versus separation distance.

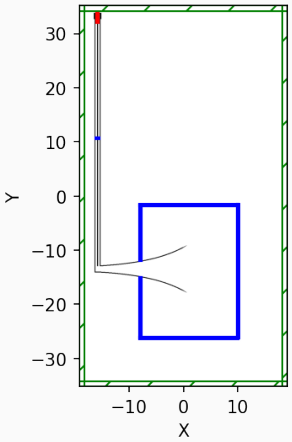

Figure 27: (Red) Gaussian or continuous source. (Black) Coaxial cable connected to RF horn. (Blue) Flux region and near-to-far regions. (Green) PML(1.0).

Let Γ be the *reflection coefficient* caused by any impedance mismatch at a given frequency (potentially complex).

$$\frac{V_r}{V_f} = \Gamma = \frac{Z_L - Z_0}{Z_L + Z_0} \tag{7}$$

The voltage standing wave ratio (VSWR) is defined in terms of $|\Gamma|$:

$$VSWR = \frac{1 + |\Gamma|}{1 - |\Gamma|} \tag{8}$$

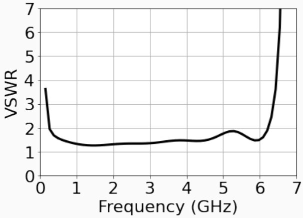

Figure 28: VSWR vs. frequency for the 2D horn.

Progress in RF Antenna Design

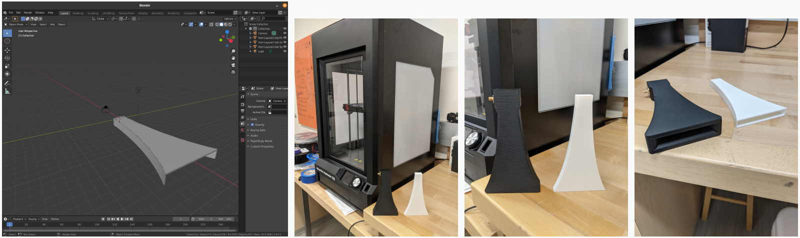

Horizontal Traces	Dimension ($X \times Y \times Z$ cm^3)	Resistance (Ω)	Resistivity (Ω cm)
Electrifi	0.2 × 10 × 0.2	3.0	0.012
Black Magic 3D	0.2 × 10 × 0.2	142.5	0.57
Proto-Pasta	0.2 × 10 × 0.2	1506	6.02

Vertical Towers	Dimension ($X \times Y \times Z$ cm^3)	Resistance (Ω)	Resistivity (Ω cm)
Electrifi	0.5 × 0.5 × 10	3.4	0.085
Black Magic 3D	0.5 × 0.5 × 10	103.6	2.59
Proto-Pasta	0.5 × 0.5 × 10	410	10.25

Figure 29: (Far left) Blender/STL files (Left) MakerBot printer (Right) Example horns (Far right) Horns front view. Black horn made with Proto Pasta.

GDSII to STL: mbalestrini/gdsiistl via GitHub.

MEEP parallelism accelerates `set_epsilon` phase of 3D horn computation.

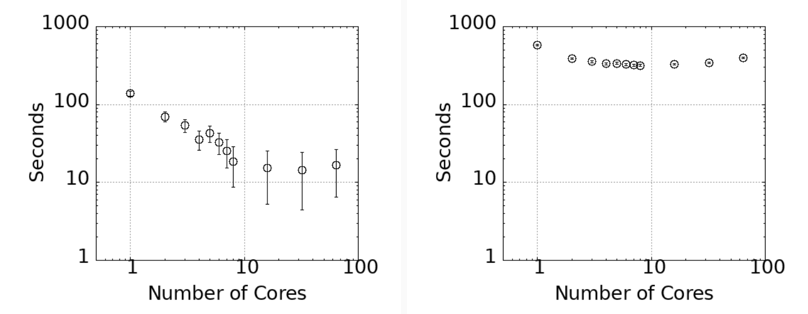

Figure 30: (Left) Time required to set epsilon versus number of cores. (Right) Total time required for total computation.

There is a growing field of research in 3D printing of RF systems.

1. Myung Jun Kim *et al* “One-step electrodeposition of copper on conductive 3D printed objects.” Additive Manufacturing **27** (2019) pp. 318-326. doi:10.1016/j.addma.2019.03.016
2. Okan Yurduseven *et al* “Computational microwave imaging using 3D printed conductive polymer frequency-diverse metasurface antennas.” IET Microwaves, Antennas and Propagation (Special Issue: Microwave Components and Antennas Based on Advanced Manufacturing Techniques), (2017) doi:10.1049/iet-map.2017.0104
3. Okan Yurduseven *et al* “3D Conductive Polymer Printed Metasurface Antenna for Fresnel Focusing.” Designs (2019), 3(3), 46. doi:10.3390/designs3030046
4. Francisco Pizarro *et al* “Parametric Study of 3D Additive Printing Parameters Using Conductive Filaments on Microwave Topologies.” IEEE Access, **7**, pp. 106814-106823, 2019, doi:10.1109/ACCESS.2019.2932912.

Conclusion

Conclusion - Contact me @ jhanson2@whittier.edu

    

1. **Background** ... *From microns to centimeters: applications of CEM in research with IceCube Gen2 and the Office of Naval Research (ONR)*
2. **Broadband RF Phased Arrays** ... *Computations of phased array designs, matching results to theoretical expectations*
3. **Variation of the Index of Refraction** ... *Ray-tracing and 3D mapping of RF phased array radiation in non-trivial media*
4. **Progress in RF Antenna Design** ... *RF antenna CAD and GDSII import, predicting antenna efficiency and radiation pattern, 3D printing of final products*
5. **Gratitude for my Colleagues** ... *Adam Wildanger, Raymond Hartig, Dane Goodman, Shaun Dunnick*

Code Examples